

Variability analysis on modal parameters of Runyang Bridge during Typhoon Masta

Jian-Xiao Mao^a, Hao Wang^{*}, Zhi-Xiang Xun^b and Zhong-Qin Zou^c

Key Laboratory of C&PC Structures of Ministry of Education, Southeast University,
No.2, Sipailou, Nanjing 210096, China

(Received September 19, 2016, Revised January 11, 2017, Accepted January 17, 2017)

Abstract. The modal parameters of the deck of Runyang Suspension Bridge (RSB) as well as their relationships with wind and temperature are studied based on the data recorded by its Structural Health Monitoring System (SHMS). Firstly, frequency analysis on the vertical responses at the two sides of the deck is carried out to distinguish the vertical and torsional vibration modes. Then, the vertical, torsional and lateral modal parameters of the deck of RSB are identified using Hilbert-Huang Transform (HHT) and validated by the identified results before RSB was opened to traffic. On the basis of this, the modal frequencies and damping ratios of RSB during the whole process of Typhoon Masta are obtained. And the correlation analysis on the modal parameters and wind environmental factors is then conducted. Results show that the HHT can achieve an accurate modal identification of RSB and the damping ratios show an obvious decay trend as the frequencies increase. Besides, compared to frequencies, the damping ratios are more sensitive to the environmental factors, in particular, the wind speed. Further study on configuring the variation law of modal parameters related with environmental factors should be continued.

Keywords: modal parameter; suspension bridge; typhoon; wind; temperature; HHT

1. Introduction

The long span suspension bridge, which is featured as flexible and low damping, is vulnerable to wind loads. The structural intrinsic dynamic properties could indicate its security status. Therefore, accurate identification of modal parameters such as frequencies and damping ratios is important for damage identification and security evaluation of long span suspension bridges (Doebbling *et al.* 1998, Ren and De Roeck 2002, Ou and Li 2010, Li *et al.* 2014). Operational modal analysis (OMA) is recommended in most situations due to its safety and economy in implementation (Peeters and De Roeck 2001, Brownjohn 2003, Kim *et al.* 2015, Spencer *et al.* 2004). The corresponding test is conducted without interrupting the traffic, and the unknown load is assumed as white noise excitation. Numerous methods for OMA of civil structures have been proposed in the literature (Feng *et al.* 1998, Brincker *et al.* 2001, Reynders 2012). Conclusions could be reached that time-frequency methods including Hilbert-Huang Transform (HHT) and Wavelet Transform (WT) are capable of analyzing nonlinear and non-stationary time

histories in low frequency domain. And the adaptive nature of HHT makes it better while the parameter choice of WT is experiential and deficient (Chen *et al.* 2004, Yan and Miyamoto 2006, Zhang *et al.* 2013).

The long suspension bridge is one kind of complicated and nonlinear structural system, and its modal parameters depend largely on the structural types and material properties. The material properties are susceptible to environmental factors including temperature, humidity and etc. Besides, the aerodynamic shape of the main girder would vary when the surrounding wind speed changes. Consequently, the uncertain environmental factors may reduce the reliability of damage identification based on the identified modal parameters. Numerous researches focused on the changeable modal parameters under different temperatures have been conducted (Ni and Hua 2005, Hua *et al.* 2007, Li *et al.* 2010, Yarnold *et al.* 2015, Wang *et al.* 2016). Conclusions are reached that temperature is the most significant environmental factor leading to the variation of structural modal frequencies. However, the relationship between the temperature and damping ratios is still not clear. Besides, researches on the comprehensive relationship between modal parameters and environments including temperature and wind are limited, especially for long suspension bridges under extreme typhoon excitations.

This paper presents a detailed research on the variability of modal parameters of Runyang Suspension Bridge (RSB) related with wind and temperature during Typhoon Masta. On the basis of the recorded structural acceleration responses recorded by the Structural Health Monitoring System (SHMS) of RSB, modal parameters including frequencies and damping ratios of the girder are identified using HHT. Then, the relation between identified modal

*Corresponding author, Professor
E-mail: wanghao1980@seu.edu.cn

^a Ph.D. Student
E-mail: jx1990@seu.edu.cn

^b M. S. Student
E-mail: 220150941@seu.edu.cn

^c M. S. Student
E-mail: zouzhongqin@seu.edu.cn

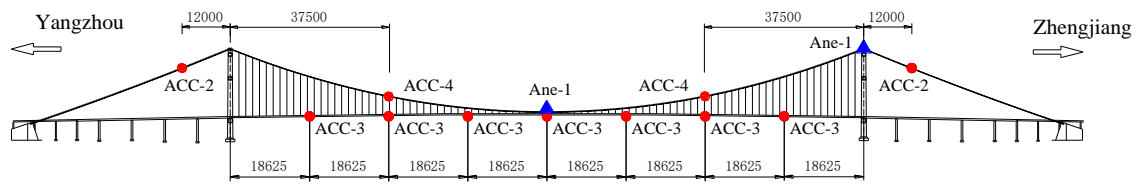


Fig. 1 ACC and ANE installed at RSB (Unit: cm)

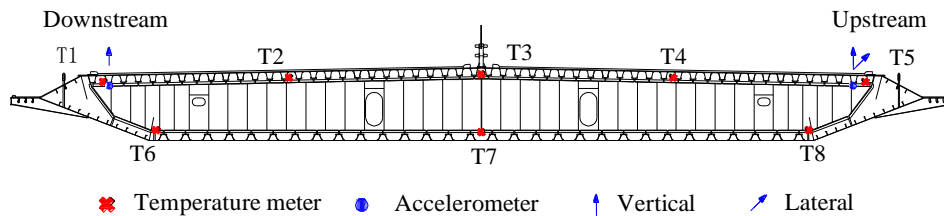


Fig. 2 Temperature meters and ACCs installed at the mid-section of the mid girder of RSB

parameters and environmental factors including temperature and wind during Typhoon Masta are analyzed. Research results can provide valuable information for the safety evaluation of the similar long suspension bridges during typhoons.

2. Engineering background and data source

2.1 Structural health monitoring of RSB

RSB, with a main span of 1490 m, was the 3rd longest bridge around the world and the longest bridge in China when it was completed in 2005. It is located in Jiangsu Province where prominent thermodynamic difference between sea and land exists. Therefore, seasonal alternating monsoon is formed and disasters such as typhoons occur frequently. Consequently, a comprehensive SHMS was installed at this bridge since it was opened to traffic. The traffic, wind, temperature, humidity at the bridge site together with its deformation and acceleration are recorded by the SHMS which aims at making a timely evaluation of its structural condition. And the sensors which aim to monitor wind, temperature and acceleration responses are shown in Figs. 1 and 2.

As shown in Fig. 1, 7 groups of capacitive single axis accelerometers (ACC), which are produced by KISTLER, are installed on the main girder. Each group of ACC consists of two vertical sensors and one lateral sensor. The two vertical sensors are installed at the two sides of the deck, respectively. And the lateral one is only installed at the upstream side. Besides, there are 4 groups of ACC on the cable. Among them, two groups of the mid span consist of two vertical and two lateral sensors, while other two at the side span consist of two lateral sensors. Measuring range of the ACC is set as -1.0 g to +1.0 g and its sampling frequency is set as 20 Hz. At the same time, two WA15 anemometers (ANE) from the Vaisala Company (USA) are installed on RSB to monitoring the situ wind environment

as its sampling frequency is set as 1 Hz. The north direction is set as 0 degree of the ANE. By the convention that positive rotation goes clockwise, east is 90°, and so on. As shown in Fig. 2, 8 temperature meters, whose sampling rate is set as 20 Hz, are installed at the mid-span section of the main girder of RSB, which aims to monitor the structural temperature of orthotropic steel deck.

2.2 Field measurement during Typhoon Masta

On August of 2005, the Typhoon Masta directly attacked Jiangsu and Zhejiang Province of China, which has caused huge economic losses. Fig. 3 exhibits the moving path of this typhoon. Nanjing, Zhenjiang and Yangzhou were located in the region where weather featured as strong wind and heavy rain. And the maximum wind scale, Beaufort scale, exceeded 12 (Gao and Wang 2008).

As shown in Fig. 3, RSB which connects Zhenjiang and Yangzhou is close to the moving path of Typhoon Masta. The SHMS of RSB recorded the whole process when the typhoon passed by. The wind velocity, structural acceleration and temperature at the mid span of RSB are continuously measured from 13:00 on August 5 to 01:00 on August 7, 2005. The recorded total 36 hours in-situ data are shown in Figs. 4 and 5, respectively. The sampling frequency of acceleration is set as 20 Hz while those of wind velocity and temperature are set as 1 Hz.



Fig. 3 The moving path of Typhoon Masta

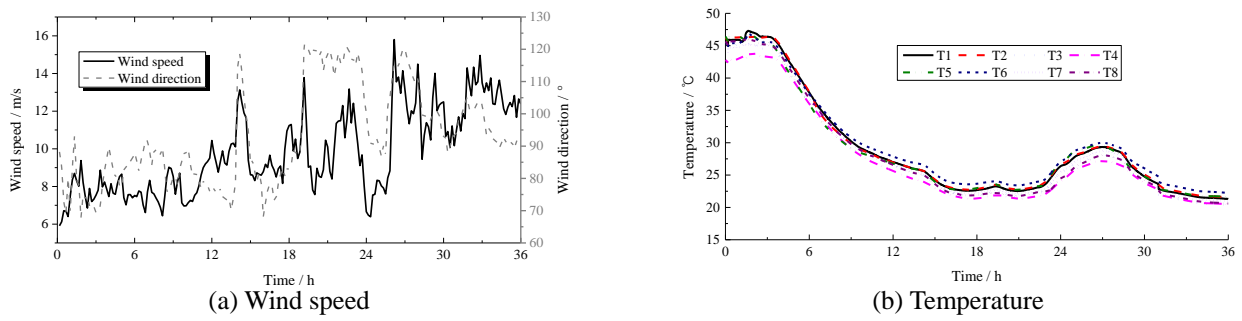


Fig. 4 Measured environmental factors at the mid span of RSB during Typhoon Masta

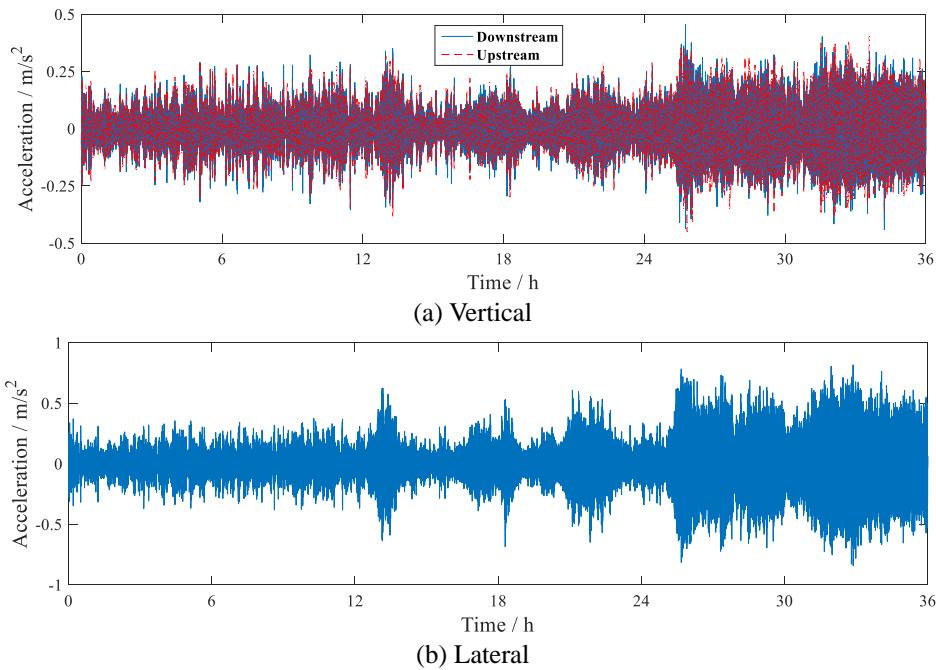


Fig. 5 Measured acceleration responses at the mid span of RSB during Typhoon Masta

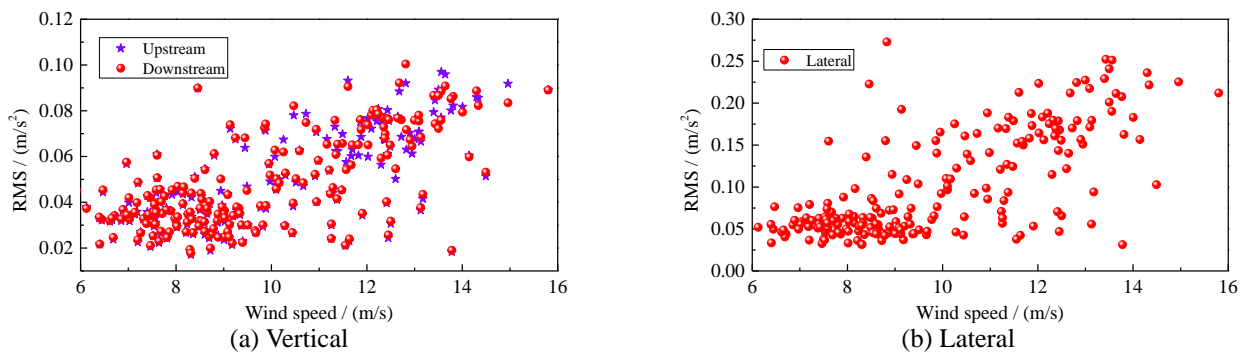


Fig. 6 Variation of acceleration RMS with the in-situ wind speed

As depicted in Fig. 4, by the approaching of Typhoon Masta, the wind speed obviously increases while the wind direction shows stronger fluctuation. Besides, the structural temperature sharply decreases with a value of larger than 20 °C. As shown in Fig. 5, the measured 3 acceleration

responses all exhibit similar variation trend with the in-situ wind speed, since there are 5 obvious peaks in both acceleration and wind speed histories. The 10-minutes root mean square (RMS) values of all the 3 acceleration responses are calculated and then scattered with the in-situ wind speed, as shown in Fig. 6.

As shown in Fig. 6, the vertical acceleration RMS values at the downstream and upstream side of the bridge deck both increase with the increase of the measured wind speed at the mid-span of RSB, although small discrepancy exist at the high wind speed range. And the increase trends of the vertical and lateral RMS values are similar with each other. By contrast, the lateral RMS values are larger than those of vertical RMS values, which shows the constrained effects in the lateral direction is weaker than those in the vertical direction.

3. Presentation of the basic theory

3.1 Modal parameter identification using HHT

For vibration signal of multiple degrees of freedom excited by the white noise force, the corresponding free decay responses can be obtained using the random decrement technique (Zhang and Song 2016). The free decay signal $x(t)$ consists of n sinusoids which can be represented as

$$x(t) = \sum_{i=1}^n x_i(t) = \sum_{i=1}^n A_i e^{-2\pi\zeta_i f_i t} \cos(2\pi f_{di} t + \theta_i) \quad (1)$$

Where A is the amplitude, θ is the phase, f is the natural frequency, $f_{di} = f_i \sqrt{1 - \zeta_i^2}$ represents the damped natural frequency, ζ is the damping ratio, i represents the i_{th} vibration mode.

The aforementioned multiple-component vibration signal can be decomposed into mono-component intrinsic mode functions (IMF) based on the empirical mode decomposition (EMD) technique (Chen *et al.* 2004).

$$x(t) = \sum_{i=1}^n c_i(t) + r_n(t) \quad (2)$$

Where c is the mono-component IMF and r is the residual which represents the measurement noise.

Filter process is usually applied to filter out the noise component. Therefore, the vibration responses of the i_{th} mode $x_i(t)$ approximate equal to the i_{th} IMF $c_i(t)$. Then, the corresponding analytical signal $z_i(t)$ can be obtained as

$$z_i(t) = x_i(t) + jy_i(t) = A_i e^{-2\pi\zeta_i f_i t} e^{j(2\pi f_{di} t + \theta_i)} \quad (3)$$

Where $y_i(t)$ is the Hilbert-Transform formation of $x_i(t)$ and defined as $\int_{-\infty}^{+\infty} \frac{x_i(\tau)}{\pi(t-\tau)} d\tau$.

According to Eqs. (1)-(3), the multi components signal can be decomposed into some single component signal in the range of concerning frequency band. And Eq. (3) can be simplified as Eq. (4)

$$z_i(t) = A_i e^{-2\pi\zeta_i f_i t} e^{j(2\pi f_{di} t + \theta_i)} = B_i(t) e^{j\varphi_i(t)} \quad (4)$$

Where $B_i(t) = A_i e^{-2\pi\zeta_i f_i t}$ and $\varphi_i(t) = 2\pi f_{di} t + \theta_i$ is the instantaneous amplitude and phase angle, respectively.

On the basis of above analysis, the modal frequency f and damping ratio ζ of the i_{th} vibration mode can be obtained according to Eq. (5).

$$\ln B_i(t) = -2\pi\zeta_i f_i t + \ln A_i \quad (5a)$$

$$\frac{d\varphi_i(t)}{dt} = 2\pi f_{di} = 2\pi f_i \sqrt{1 - \zeta_i^2} \quad (5b)$$

3.2 Principal component analysis

Principal component analysis (PCA) is a linear multi-variable statistics method for data analysis, aiming to extract relevant information from redundant data sets (Shlens 2014). PCA is first introduced by Pearson (1901) and then applied into biology, chemistry and civil engineering (Nazarian *et al.* 2016). In this paper, the PCA is used to extract the main featured components of the structural temperature measured by the 8 temperature meters installed at the mid-section of the main girder, including the variation trend of mean temperature and temperature difference of the main girder). The basic theory of PCA utilized in this research is summarized as follows.

Given a measured data set of l variables, $x = [x_1; L; x_l]$, where each x_i includes n observations, a linear transformation is conducted so as to get a new representation u instead of x

$$u = ax \quad (6)$$

Where u is a new representation of the original data set, $a = \{a_1, a_2, \dots, a_l\}^T$ is a matrix that transforms x into u . The row vectors $\{a_1, a_2, \dots, a_l\}$ in the linear transformation are called principal components of x . Then, the constructed value x' can be obtained according to Eq. (7) according to the assumption that a is an orthonormal matrix.

$$x' = a^T u \quad (7)$$

The property of eigenvector decomposition is used to solve PCA as proposed by Shlens (2014). In the solution, two new matrixes CX and CU are defined as

$$CX = \frac{1}{n} xx^T \quad (8)$$

$$CU = \frac{1}{n} uu^T \quad (9)$$

Then, the principal components of x are eigenvectors of CX , and the i_{th} diagonal value of CU is the variance of x along a_i .

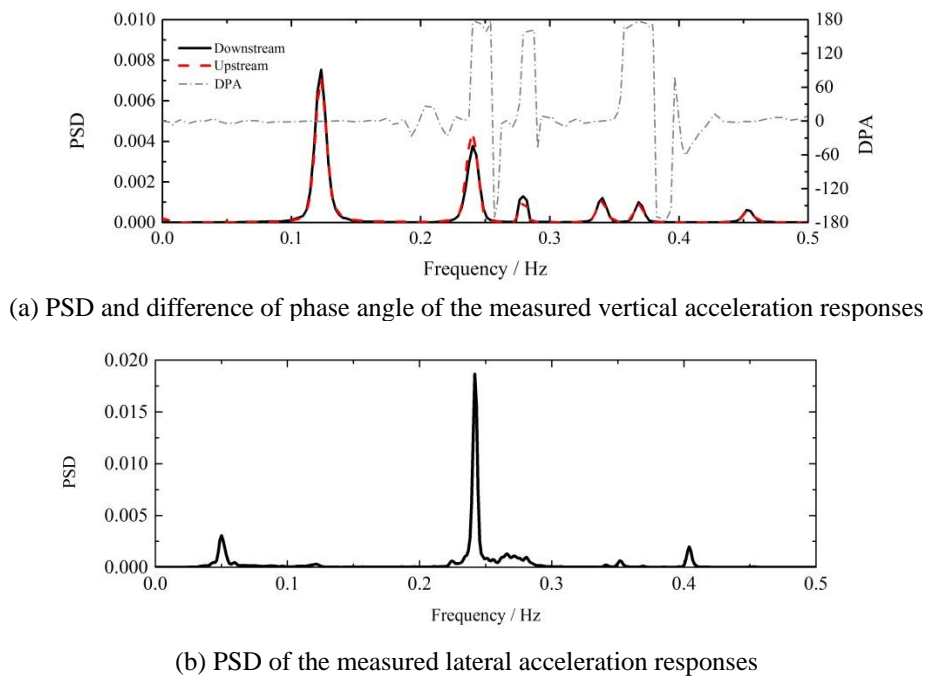


Fig. 7 Frequency analysis of the measured acceleration responses at the mid-span

Table 1 Separated mode types of RSB based on PSD and DPA analysis

Sensor direction		Vertical						Lateral		
Frequency	Measured	0.1229	0.2402	0.2793	0.3407	0.3687	0.4525	0.0501	0.2417	0.4041
(Hz)	FEA	0.1173	0.2238	0.2874	0.3383	0.3442	0.4662	0.0537	-	-
	DPA	-0.32	174.84	152.47	0.00	175.86	-0.47	-	-	-
	Mode type	V1	T1	T2	V2	T3	V3	L1	LCT1	L2

4. Modal parameter identification of RSB

4.1 Frequency analysis of measured acceleration

Traditionally, the vertical acceleration of the bridge deck is acquired by the summation of the two measurements at the upstream and downstream, respectively, while the torsional acceleration acquired by the difference of the two measurements (Wang *et al.* 2016). In this study, the vertical and torsional vibration modes are separated according to the power spectrum density (PSD) and the difference of phase angle (DPA) of the acceleration measurements at the two sides of the bridge deck, as shown in Fig. 7(a). The vertical bending mode is recognized as DPA corresponding to the picked peak frequency equals to 0 degree, while the torsional mode recognized as the corresponding DPA equals to ± 180 degree. Besides, the PSD of the lateral bending acceleration responses is also calculated, as shown in Fig. 7(b).

As shown in Fig. 7, 6 vertical/torsional modes together with 3 lateral modes could be picked at the range of

0-0.5 Hz. According to the picked DPAs at the 6 peak-frequency points, the vertical and torsional modes are separated with each other successfully. The separated results are listed in Table 1 and then compared with the finite element analysis (FEA) results calculated by Wang *et al.* (2010). In the three-dimensional finite element model of RSB established by ANSYS, the deck, the central buckle and the towers were simulated by beam elements (BEAM4) with six degrees of freedom (DOFs) for each node. The main cables and the suspenders were simulated by three-dimensional linear elastic truss elements (LINK10) with three DOFs for each node. The pavement and the railings on the steel box girder were simulated by mass elements (MASS21) without rigidity. LANCZOS eigenvalue solver is adopted to conduct the modal analysis of RSB. The FEA-based modal frequencies listed in Table 1 and the vibration shapes shown in Fig. 8 are used to validate the determined mode types.

As listed in Table 1, 3 vertical and 3 torsional modes are clearly determined based on PSD and DPA analysis. The frequencies and the corresponding determined modal types agree well with the FEA-based modal vibration shapes shown in Fig. 8. As for the measured lateral responses, 3

modes could be found according to its PSD. However, only the identified first-order frequency, which is 0.0501 Hz, could match the FEA results 0.0537 Hz. The identified lateral second-order frequency LCT1 (0.2417 Hz) is approximately the same with the first torsional mode T1 (0.2402 Hz). Consider that the torsional vibration could lead to the lateral and vertical vibration responses at the two sides of the deck, upstream and downstream. For better measure the lateral acceleration of the bridge deck, it is advised to average the two measurements at the two sides to eliminate the torsional vibration component. However, there is only one lateral acceleration sensor installed on the upstream side of the mid-span of RSB, which makes the lateral vibration histories do contain the torsional components.

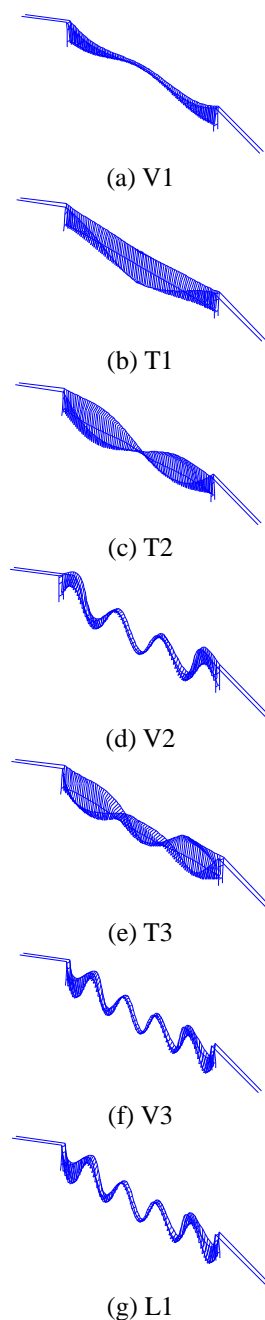


Fig. 8 FEA-based modal vibration shapes of RSB

4.2 HHT-based modal parameter identification

The identification of the vertical bending modal parameters is selected as the example to explain the identification procedure. The vertical vibration responses at the mid-span of the deck of RSB are acquired by the summation of the two measurements at the upstream and downstream. Then, the digital Butterworth band-pass filter together with the EMD is utilized to get the mono-component time history, as shown in Fig. 9. The band-pass filter is designed using infinite impulse response (IIR) Filter in Matlab with no more than 2 dB of passband ripple and at least 50 dB of attenuation in the stopband.

The calculated Hilbert spectrum of the 3 mono-component vertical time histories shown in Fig. 10 validates the accuracy of decomposition method. After the mono-component acceleration responses are acquired, the random decrement technique (RDT) is used to eliminate the forced vibration components (Zhang and Song 2016). The parameters chosen for the RDT procedure are as follows. The size of the subsample data is 2,048 points, with a time length of 102.4s. The selection rules of optimal initial displacement are as follows: 1) Guarantee a sufficient number of subsamples by setting the maximum initial displacement; 2) Preserve enough signal power by setting the minimum initial displacement; 3) The optimal initial displacement should ensure the independence between subsamples. Finally, 1.5σ (σ denotes the standard deviation of sample data) is selected for the latter analysis and was examined appropriate by Wang *et al.* (2016). Therefore, the corresponding free vibration decay responses shown in Fig. 11 are acquired.

Since the free vibration decay responses of each mono-component time history are acquired, the Hilbert transform is utilized to get the corresponding analytic signals. Its instant amplitude and phase angle are calculated according to Eq. (4). Then, the least squared method is used to fit the acquired amplitude and phase angle shown in Fig. 12. In order to reduce affection of end effects during EMD procedure, 20 data points at the head and tail of the instant amplitude and phase angle are cut to make a better linear fit. Therefore, the modal parameters of the first vertical bending mode are identified. The frequency is 0.1214 Hz and the damping ratio is 1.43%.

On the basis of this, the other vertical, torsional and lateral bending modes are identified as listed in Table 2, where Ref represents the identified modal parameters by Wang *et al.* (2010) for comparison.

It can be found that the HHT-based modal frequencies are identical with those in Ref and the damping ratios are also similar with those values in Ref. However, the conclusion can't be guaranteed for the parameters of the torsional modes. There are obvious differences between the HHT-based parameters and those values in Ref, especially for damping ratios. The modal test of Ref was conducted before RSB was opened to traffic, and no vehicle load excited the bridge deck at that time. The traffic load together with the long operation of RSB may lead to the variation of the torsional frequencies which could make the corresponding damping ratios larger.

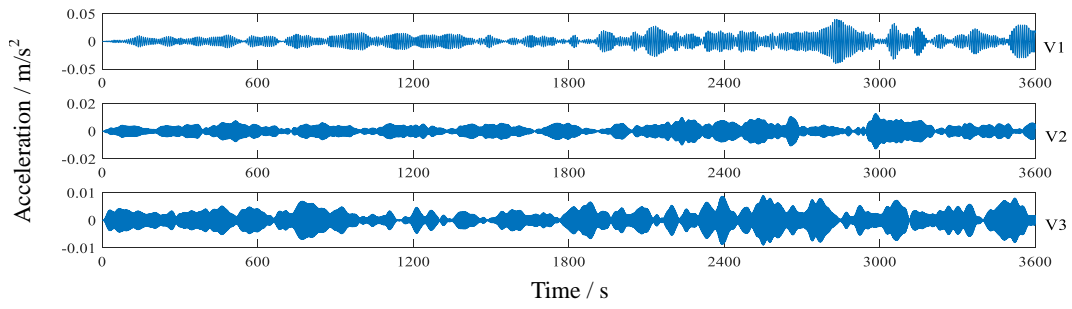


Fig. 9 First 3 mono-component time histories of the vertical acceleration responses

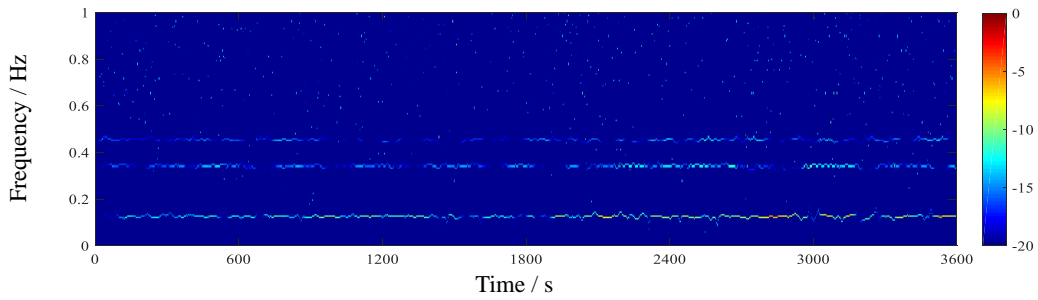


Fig. 10 Hilbert spectrum of the 3 mono-component vertical time histories

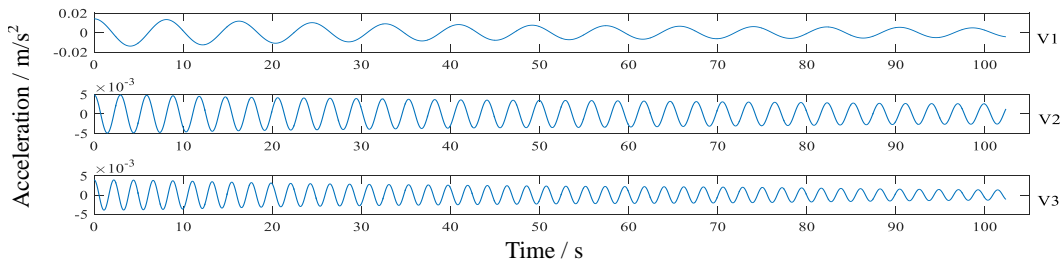


Fig. 11 Free vibration decay responses of the 3 mono-component vertical time histories

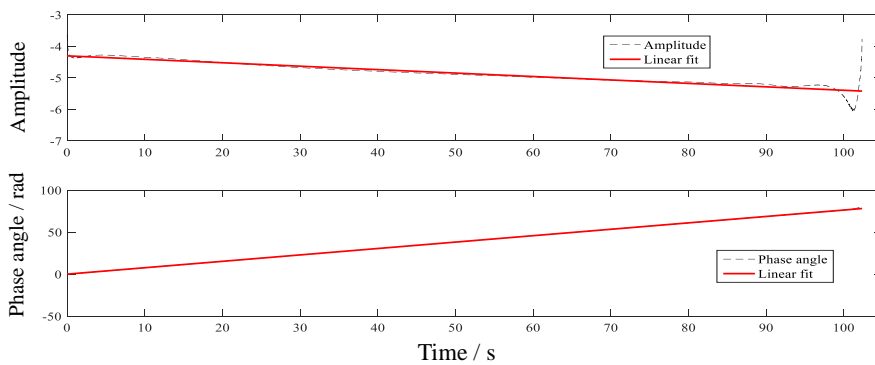


Fig. 12 The amplitude and phase angle of free vibration decay responses

Table 2 Identified modal parameters using HHT method

Modal parameter		Vertical			Torsional			Lateral		
		V1	V2	V3	T1	T2	T3	L1	LCT1	L2
Frequency (Hz)	HHT	0.1214	0.3405	0.4534	0.2418	0.2803	0.3695	0.0507	0.2418	0.4038
	Ref	0.1221	0.3418	-	0.2398	0.3098	0.3711	0.0586	-	-
Damping ratio	HHT	1.43%	0.29%	0.35%	0.26%	0.84%	0.18%	3.96%	0.32%	0.19%
	Ref	0.97%	0.66%	-	1.59%	1.01%	0.80%	2.20%	-	-

5. Analysis of modal parameters of RSB during Typhoon Masta

5.1 Temperature analysis based on PCA

Since there are 8 steel thermometers installed in the mid span of RSB, PCA is conducted on the 8 pairs of temperature measurements to extract predominant feature vectors. Table 3 summarizes the eigenvalues of covariance matrix for each temperature data set. Then, the 1st PC is constructed according to Eq. (7). The constructed value is compared with the mean value of all measurements shown in Fig. 13.

It can be seen from table 3 that the first PC accounts for 99.822% of the total variance. Conclusions could be drawn that the measured temperature records are strongly correlated. As shown in Fig. 13, the constructed value agrees well with the mean value, which validates the correctness of the PCA again. The constructed temperature value is then utilized to analyze the correlation between modal parameters and temperatures.

5.2 Correlation analysis of the identified modal parameters during Typhoon Masta

Based on the above HHT-based method, the modal parameters during the total 36 hours, when Typhoon Masta passed by, are identified in each half an hour. The identified modal parameters including frequencies and damping ratios are plotted in Fig. 14(a). The mean values of modal frequency and damping ratio each vibration modes are compared with the identified modal parameters of Golden Gate Bridge (Abdel-Ghaffar 1985) and Tsing Ma Bridge (Qin *et al.* 2001).

Table 3 Eigenvalues of Covariance Matrix for Temperature

Number	Eigenvalues	Proportion of variance	Cumulative proportion
1	459.503	99.822	99.822
2	0.568	0.124	99.946
3	0.133	0.029	99.975
4	0.056	0.012	99.987
5	0.028	0.006	99.993
6	0.020	0.004	99.997
7	0.010	0.002	99.999
8	0.003	0.001	100.000

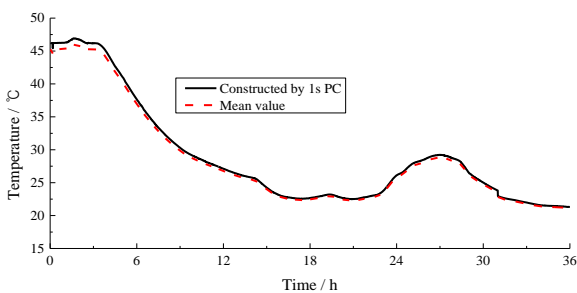


Fig. 13 Constructed temperature value by the 1st PC during Typhoon Masta

It could be seen that both the damping ratios of RSB and Golden Gate Bridge decrease with the increase of the frequencies, while those of the Tsing Ma Bridge aren't featured as such obvious phenomenon. Besides, the damping ratios of the Golden Gate Bridge are larger than those of the other two bridges since it has a shorter main span of 1280 m and two stiffening truss with better damping. Then, the linear least square method is applied to fit the relation between natural logarithm of damping ratios and original values of frequencies as shown in Fig. 14(b). It can be seen that both of natural logarithm values of damping ratios of RSB and Golden Gate Bridge show a linear decrease as the frequencies increase.

The Mean Value (MV) and Standard Deviation Value (SDV) of the each vibration mode during the 36 hours are summarized in Table 4 where Coefficient of Variation (CV) is defined as SDV/MV.

As shown in Table 4, the CVs of damping ratios during Typhoon Masta are larger than those of the frequencies, which indicate that damping ratios is more vulnerable to the changing environment than the frequencies. Therefore, the Pearson correlation coefficients (Kendall 1979) between the identified parameters and environmental factors, which include the temperature constructed by the 1st PC, wind speed and wind direction, are calculated in Table 5 and Table 6, respectively. For two variables (*A* and *B*) with *N* scalar observations, their Pearson correlation coefficient $\rho(A,B)$ is defined as

$$\rho(A,B) = \frac{1}{N-1} \sum_{i=1}^N \left(\frac{A_i - \mu_A}{\sigma_A} \right) \left(\frac{B_i - \mu_B}{\sigma_B} \right) \quad (10)$$

Where μ_A and σ_A are the mean and standard deviation of *A*, respectively, and μ_B and σ_B are the mean and standard deviation of *B*.

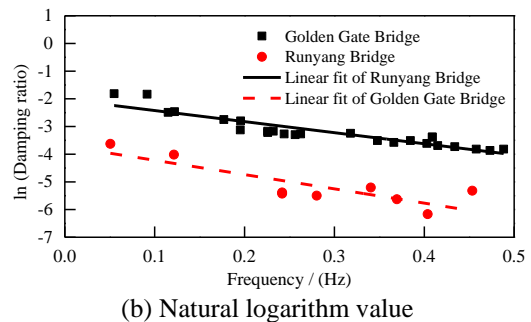
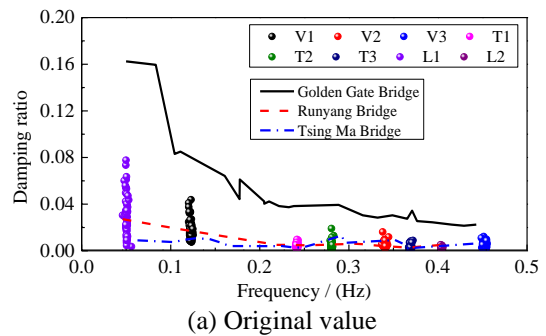


Fig. 14 Identified damping ratios and frequencies of RSB during Typhoon Masta

Table 4 Statistical analysis of the identified modal parameters during typhoon

Mode		Frequency			Damping ratio		
		1 st	2 nd	3 rd	1 st	2 nd	3 rd
Vertical	MV (Hz)	0.1225	0.3403	0.4525	1.80%	0.55%	0.49%
	SDV (Hz)	0.0011	0.0012	0.0015	0.84%	0.24%	0.21%
	CV	0.89%	0.37%	0.33%	46.79%	42.88%	42.81%
Torsional	MV (Hz)	0.2417	0.2807	0.3693	0.44%	0.41%	0.36%
	SDV (Hz)	0.0006	0.0005	0.0008	0.19%	0.31%	0.19%
	CV	0.25%	0.19%	0.21%	43.95%	74.71%	51.66%
Lateral	MV (Hz)	0.0505	0.4042	-	2.66%	0.21%	-
	SDV (Hz)	0.0013	0.0005	-	1.79%	0.11%	-
	CV	2.62%	0.12%	-	67.20%	51.50%	-

Table 5 Correlation coefficients between frequencies and environmental factors

Mode \ Factors	V1	V2	V3	T1	T2	T3	L1	L2
Temperature	-0.03	-0.13	-0.03	0.13	0.06	-0.36	0.04	-0.26
Wind Speed	-0.09	0.01	-0.13	-0.34	-0.02	0.12	0.01	0.24
Wind Direction	-0.08	0.02	-0.02	-0.16	-0.05	0.09	0.02	0.16

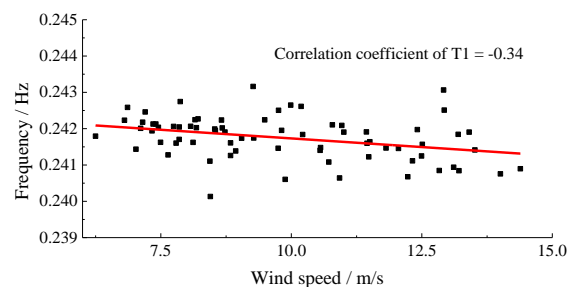
Table 6 Correlation coefficients between damping ratios and environmental factors

Mode \ Factors	V1	V2	V3	T1	T2	T3	L1	L2
Temperature	-0.24	-0.19	-0.24	-0.02	0.39	-0.49	0.20	-0.16
Wind Speed	0.46	0.26	0.29	0.41	-0.17	0.54	-0.55	0.27
Wind Direction	0.26	0.11	0.15	0.13	-0.16	0.38	-0.39	0.17

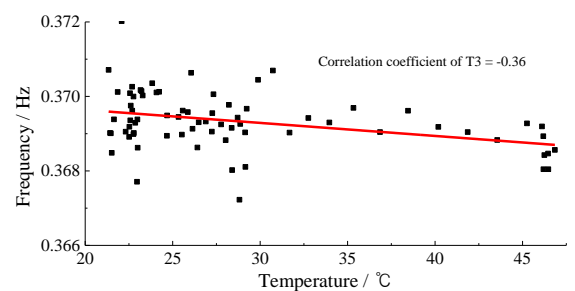
As shown in Tables 5 and 6, it could be concluded that the vertical bending frequencies show a negative correlation with the temperature, while its damping ratios show a positive correlation with the wind speed at the range of 6-15 m/s. However, the modal parameters of the lateral and torsional modes don't obey the same law and further studies need to be continued.

According to the correlation coefficients in Tables 5 and 6, the identified frequencies of most vibration modes have smaller correlation with temperature, wind speed and wind direction, compared with the identified damping ratios. The maximum coefficients of wind speed and temperature on damping ratios exceed -0.55 and -0.49, while those on frequencies are -0.34 and -0.36, respectively. And the corresponding variation trend is shown in Figs. 15 and 16.

Conclusions could be reached that the modal frequencies, correlated with structural stiffness, decrease as the increase of the environmental temperature. Modal damping ratios are more complex correlated with the temperature and wind speed. As for the vertical and torsional bending modes, the damping ratios increase with the wind speed but decrease with the temperature.



(a) Wind speed



(b) Temperature

Fig. 15 Variations of identified frequencies with half-hourly environmental factors

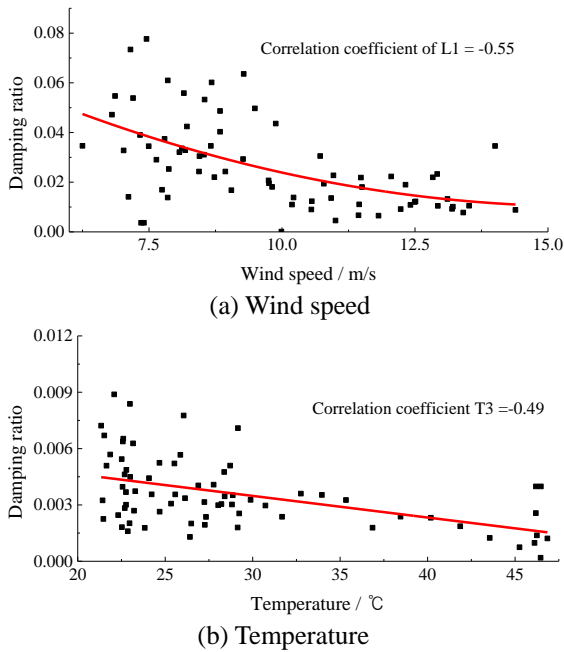


Fig. 16 Variations of identified damping ratios with half-hourly environmental factors

Especially, the damping ratio of L1 decreases as the wind speed increases. Further researches should be conducted to investigate the intricate mechanism of action between modal parameters and environmental factors especially the difference for different vibration modes.

6. Conclusions

This paper elaborates the time-frequency HHT-based modal parameter identification method and its application on a real large suspension bridge (RSB). Firstly, the frequency analysis on the vertical responses at the two sides of the deck is carried out to distinguish the vertical and torsional vibration modes. Then, the Butterworth band-pass filter together with the EMD is utilized to get the mono-component time history, and the RDT method is applied to get decay responses which could accurately represent the modal parameter and damping ratio. On the basis of this, the modal parameter of each half an hour during the whole process of Typhoon Masta is identified. The correlation of the modal parameters on wind speed and temperature is investigated. The main conclusions are as follows:

- According to the PSD and the difference of phase angle of the two acceleration measurements at the bridge deck of the mid-span of RSB, 6 vertical/torsional modes are successfully separated, respectively.
- The HHT-based method can achieve a reliable identification of modal parameters of RSB which is featured as low frequency and low damping. And the comparison between the HHT-based identification results and Ref indicates that the traffic load together with the long operation of RSB may lead to the variation of the torsional frequencies, making the corresponding damping ratios larger.

- The vertical bending frequencies show a negative correlation with the temperature, while its damping ratios show a positive correlation with the wind speed at the range of 6-15 m/s.

- The damping ratios of most vibration modes have larger correlation with temperature, wind speed and wind direction, compared with the identified frequencies.

- The damping ratios of RSB decrease with the increase of the frequencies. Especially, its natural logarithm values show a linear decrease as the frequencies increase.

The above conclusions could provide some useful references for status evaluation of long-span bridges under strong typhoon. However, more comprehensive researches need to be conducted in order to configure the variation law of modal parameters during extreme weather.

Acknowledgments

The research described in this paper was financially supported by the National Basic Research Program of China (973 Program) (No. 2015CB060000), the National Natural Science Foundation of China (No. 51378111 and 51438002), the Program for New Century Excellent Talents in University of Ministry of Education (No. NCET-13-0128) and the Fok Ying-Tong Education Foundation for Young Teachers in the Higher Education Institutions of China (No. 142007). The authors also thank the help from Jiangsu Health Monitoring Data Center for Long-span Bridges and the Structural Health Monitoring Institute in Southeast University.

References

- Abdel-Ghaffar, A.M. and Scanlan, R.H. (1985), "Ambient vibration studies of golden gate bridge: I. Suspended structure", *J. Eng. Mech. - ASCE*, **111**(4), 463-482.
- Brincker, R., Zhang, L. and Andersen, P. (2001), "Modal identification of output-only systems using frequency domain decomposition", *Smart Mater. Struct.*, **10**(3), 441.
- Brownjohn, J.M.W. (2003), "Ambient vibration studies for system identification of tall buildings". *Earthq. Eng. Struct. D.*, **32**(1), 71-95.
- Chen, J., Xu, Y.L. and Zhang, R.C. (2004), "Modal parameter identification of Tsing Ma suspension bridge under Typhoon Victor: EMD-HT method", *J. Wind Eng. Ind. Aerod.*, **92**(10), 805-827.
- Doebeling, S.W., Farrar, C.R. and Prime, M.B. (1998), "A summary review of vibration-based damage identification methods", *Shock Vib. Digest*, **30**(2), 91-105.
- Feng, M.Q., Kim, J.M. and Xue, H. (1998), "Identification of a dynamic system using ambient vibration measurements", *J. Appl. Mech.*, **65**(4), 1010-1021.
- Gao, F. and Wang, H.Q. (2008), "Numerical simulation and structure analysis of typhoon MATSA (0509)", *Acta Scientiarum Naturalium Universitatis Pekinensis*, **44**(3), 385-390. (In Chinese)
- Hua, X.G., Ni, Y.Q., Ko, J.M., et al. (2007), "Modeling of temperature-frequency correlation using combined principal component analysis and support vector regression technique", *J. Comput. Civil Eng.*, **21**(2), 122-135.

- Kendall, M.G. (1979), *The Advanced Theory of Statistics (4th Ed)*. London, Macmillan.
- Kim, R.E., Moreu, F. and Spencer, Jr. B.F. (2015), "System identification of an in-service railroad bridge using wireless smart sensors", *Smart Struct. Syst.*, **15**(3), 683-698. BS
- Li, H., Li, S.L., Ou, J.P., et al (2010), "Modal identification of bridges under varying environmental conditions: temperature and wind effects", *Struct. Control Health Monit.*, **17**(5), 495-512.
- Li, J., Ruiz-Sandoval, M., Spencer, Jr. B.F., et al. (2014), "Parametric time-domain identification of multiple-input systems using decoupled output signals", *Earthq. Eng. Struct. D.*, **43**(9), 1307-1324.
- Nazarian, E., Ansari, F., Zhang, X., et al (2016), "Detection of tension loss in cables of cable-stayed bridges by distributed monitoring of bridge deck strains", *J. Struct. Eng. - ASCE*, **142**(6), 04016018.
- Ni, Y.Q., Hua, X.G., Fan, K.Q., et al (2005), "Correlating modal properties with temperature using long-term monitoring data and support vector machine technique", *Eng. Struct.*, **27**(12), 1762-1773.
- Ou, J.P. and Li, H. (2010), "Structural health monitoring in mainland China: review and future trends", *Struct. Health Monit.*, **9**(3), 219-231.
- Pearson, K. (1901), "On lines and planes of closest fit to systems of points in space", *Philosoph. Mag.*, **2**(6), 559-572.
- Peeters, B. and De Roeck, G. (2001), "Stochastic system identification for operational modal analysis: a review", *J. Dynam. Syst. Meas. Control*, **123**(4), 659-667.
- Peterson, L.D., Bullock, S.J. and Doebling, S.W. (1996), "The statistical sensitivity of experimental modal frequencies and damping ratios to measurement noise", *Int. J. Anal. Exp. Modal Anal.*, **11**(1), 63-75.
- Qin, Q., Li, H.B., Qian, L.Z., et al. (2001), "Modal identification of Tsing Ma bridge by using improved eigensystem realization algorithm", *J. Sound Vib.*, **247**(2), 325-341.
- Ren, W.X. and De Roeck, G. (2002), "Structural damage identification using modal data. I: Simulation verification", *J. Struct. Eng. - ASCE*, **128**(1), 87-95.
- Reynders, E. (2012), "System identification methods for (operational) modal analysis: review and comparison", *Arch. Comput. Method. E.*, **19**(1), 51-124.
- Shlens, J. (2014), A tutorial on principal component analysis [Online]. Available: <http://arxiv.org/abs/1404.1100>.
- Spencer, Jr. B.F., Ruiz-Sandoval, M.E. and Kurata, N. (2004), "Smart sensing technology: opportunities and challenges", *Struct. Control Health Monit.*, **11**(4), 349-368.
- Wang, H., Li, A.Q. and Li, J. (2010). "Progressive finite element model calibration of a long-span suspension bridge based on ambient vibration and static measurements", *Eng. Struct.*, **32**(9), 2546-2556.
- Wang, H., Mao, J.X., Huang, J.H., et al (2016), "Modal identification of Sutong cable-stayed bridge during typhoon Haikui using wavelet transform method", *J. Perform. Constr. Fac.*, **30**(5), 04016001.
- Yan, B. and Miyamoto, A. (2006), "A comparative study of modal parameter identification based on wavelet and Hilbert-Huang transforms", *Comput.- Aided Civil Infrastruct. Eng.*, **21**(1), 9-23.
- Yarnold, M.T., Moon, F.L. and Aktan, A.E. (2015), "Temperature-based structural identification of long-span bridges", *J. Struct. Eng. - ASCE*, **141**(11), 04015027.
- Zhang, J., Yan, R.Q. and Yang, C.Q. (2013), "Structural modal identification through ensemble empirical modal decomposition", *Smart Struct. Syst.*, **11**(1), 123-134.
- Zhang, Y. and Song, H.W. (2016). "Non-overlapped random decrement technique for parameter identification in operational modal analysis", *J. Sound Vib.*, **366**, 528-543.